Carbonate System Parameters of an Algal-dominated Reef along West Maui

Nancy G. Prouty[1], Kimberly K. Yates[2], Nathan Smiley[2], Chris Gallagher[3], Olivia Cheriton[1], and Curt D. Storlazzi[1]

[1]U.S. Geological Survey, Coastal and Marine Geology, Pacific Coastal and Marine Science Center, Santa Cruz, CA 95060
[2] U.S. Geological Survey, Coastal and Marine Geology, St. Petersburg Coastal and Marine Science Center 600 4th Street South, St. Petersburg, FL 33701
[3] University of California, Santa Cruz, Santa Cruz, CA 95060

Correspondence to: Nancy G. Prouty nprouty@usgs.gov

Abstract

Constraining coral reef metabolism and carbon chemistry dynamics are fundamental for understanding and predicting reef vulnerability to rising coastal CO_2 concentrations and decreasing seawater pH. However, few studies exist along reefs occupying densely inhabited shorelines with known input from land-based sources of pollution. The shallow coral reefs off Kahekili, West Maui, are exposed to nutrient-enriched, low-pH submarine groundwater discharge (SGD) and are particularly vulnerable to the compounding stressors from land-based sources of pollution and lower seawater pH. To constrain the carbonate chemistry system, nutrients and carbonate chemistry were measured along the Kahekili reef flat every 4 h over a 6-d sampling period in March 2016. Abiotic process - primarily SGD fluxes - controlled the carbonate chemistry adjacent to the primary SGD vent site, with nutrient-laden freshwater decreasing pH levels and favoring undersaturated aragonite saturation (Ω_{arag}) conditions. In contrast, diurnal variability in the carbonate chemistry at other sites along the reef flat was driven by reef community metabolism. Superimposed on the diurnal signal was a transition during the second sampling period to a surplus of total alkalinity (TA) and dissolved inorganic carbon (DIC) compared to ocean end-member TA and DIC measurements. A shift from positive net community production and positive net community calcification to negative net community production and negative net community calcification was identified. This transition occurred during a period of increased SGD-driven nutrient loading, lower wave height, and reduced current speeds. This detailed study of carbon chemistry dynamics highlights the need to incorporate local effects of nearshore oceanographic processes into predictions of coral reef vulnerability and resilience.

1. Introduction

Coral reefs provide critical shoreline protection and important ecosystem services, such as marine habitat, and support local economies through tourism, fishing, and recreation (Hughes et al., 2003; Ferrario et al., 2014). However, coral reefs are being threatened by global climate change processes, such as increasing temperatures, sea-level rise and ocean acidification (OA, caused by uptake of atmospheric carbon dioxide into the ocean (Orr et al., 2005). These effects are often compounded by local stressors such as over-fishing, sedimentation, land-based sources of pollution and coastal acidification (Knowlton and Jackson, 2008) that can result from freshwater inflow, eutrophication, and/or coastal upwelling. These stressors can lead to a decrease in reef health by removing grazing fish, decreasing calcification rates, and increasing nutrient and contaminant concentrations, thereby shifting the balance between reef accretion and erosion. However, isolating the effects of these stressors is difficult without establishing the biological and physical controls on community

calcification and production. This is particularly challenging for coral reefs adjacent to densely inhabited shorelines, where freshwater fluxes can deliver excess nutrients. In turn, this can lead to coastal acidification caused by eutrophication and enhanced respiratory processes that release CO_2 and increase coastal water acidity (e.g., Cai et al., 2011; Strong et al., 2014), outbreaks of harmful algal blooms (Anderson et al., 2002), and decreased coral abundance and diversity (Fabricius, 2005;Lapointe et al., 2005). In many cases, eutrophication can alter ecosystem function and structure by shifting reefs from coral- to algae-dominated (Howarth et al., 2000; Andrefouet et al., 2002; Hughes et al., 2007). Changes in community structure can have profound impacts on coral reef metabolism and reef carbon chemistry dynamics (e.g. Page et al., 2016), which are ultimately linked to reef health and the ability to predict future responses to rising pCO_2 levels (Andersson and Gledhill, 2013). Understanding the local drivers of ecosystem function and reef community metabolism is critical for gauging the susceptibility of the reef ecosystem to future changes in ocean chemistry.

Numerous efforts have been conducted along west Maui, Hawaii, USA, to characterize and quantify submarine groundwater discharge (SGD) and associated nutrient input (Dailer et al., 2010;Dailer et al., 2012;Glenn et al., 2013;Swarzenski et al., 2013;Swarzenski et al., 2016;Silbiger et al., 2017), which may influence reef metabolism and community composition by changing coastal water quality. Building upon these studies, we present a comprehensive study to characterize the carbonate system parameters from the reefs in this area. The carbonate chemistry system is sensitive to changes in photosynthesis, respiration, calcification, and calcium carbonate ($CaCO_3$) dissolution, and can be characterized by measuring total alkalinity (TA), dissolved inorganic carbon (DIC), pH, pCO_2, nutrients, salinity, and temperature. Analysis of these parameters yields valuable information on ratios of net community calcification and production, and can be used to identify biological and physical drivers of reef health and ecosystem function (Silverman et al., 2007; Shamberger et al., 2011; Lantz et al., 2014; Albright et al., 2015; Muehllehner et al., 2016; DeCarlo et al., 2017; Richardson et al., 2017; Cyronak et al., 2018). This is particularly important given growing concern that coastal and ocean acidification may shift reef ecosystems from calcification to dissolution by the mid to end of the century (Silverman et al., 2009; Andersson and Gledhill, 2013) with an overall reduction in calcification rates and increase in dissolution rates (Shamberger et al., 2011; Shaw et al., 2012; Bernstein et al., 2016) that can contribute to reef collapse (Yates et al., 2017).

The health of many of Maui's coral reefs has been declining rapidly (Rodgers et al., 2015), with recent coral bleaching events leading to increased coral mortality (Sparks et al., 2016). The decline in coral

cover along the shallow coral reef at Kahekili has been observed for decades (Wiltse, 1996; Ross et al., 2012), along with a history of macro-algal blooms (Smith et al., 2005). The shift in benthic cover from abundant corals to turf- or macro-algae (primarily *Ulva fasciata*) and increased rates of coral bioerosion have been linked to input of nutrient-rich water via wastewater injection wells (Dailer et al., 2010;Dailer et al., 2012; Prouty et al. 2017a). Treated wastewater is injected through these wells into groundwater that flows toward the coast where it emerges on the reef through a network of small seeps and vents (Glenn et al., 2013;Swarzenski et al., 2016). Changes in coastal water quality observed off west Maui can impact the balance of production of $CaCO_3$ skeletons by calcifying algae and animals on the reef, cementation of sand and rubble, and $CaCO_3$ breakdown and removal that occurs through bioerosion, dissolution, and offshore transport. Here, a high-resolution seawater sampling study was conducted to constrain the carbonate chemistry system and evaluate the biological and physical processes altering reef health along the shallow coral reef at Kahekili in Kaanapali, west Maui, Hawaii, USA (Fig. 1). This study characterizes the diurnal and multi-day variability of coral reef carbonate chemistry along a tropical fringing reef adjacent to a densely inhabited shoreline with known input from land-based sources of pollution, and identifies the controls on carbon metabolism. Ultimately, understanding carbonate system dynamics is essential for managing compounding effects from local stressors.

2. Methods

2.1 Study Site

The benthic habitat along the shallow reef at Kahekili in Kaanapali, West Maui (Fig. 1) consists of aggregate reef, patch reef, pavement, reef rubble and spur and groove (Cochran et al., 2014), with persistent current flow to the south (Storlazzi and Jaffe, 2008). Only 51% of the hardbottom at Kahekili is covered with at least 10% live coral, with the remaining hardbottom consisting of aggregate reef, spur-and-groove, patch reefs, pavement, and reef rubble (Cochran et al., 2014). The shallow fore reef experiences algae blooms in response to inputs of nutrient-rich water via wastewater injection wells (Dailer et al., 2010;Dailer et al., 2012). Groundwater inputs occur from both natural sources (rainfall and natural infiltration) and from artificial recharge (irrigation and anthropogenic wastewater). The inland Wailuku Basalt, consisting of a band of unconsolidated sediment along the coast and a small outcrop of Lahaina Volcanics, dominates the geology of the area surrounding the study site, controlling the flow of groundwater. Mean annual precipitation rates are up to 900 cm yr^{-1} (Giambelluca et al., 2013), with natural recharge the greatest in the interior mountains.

2.2 Field Sampling

Two intensive sampling periods were carried out during the 6-d period between 2016-03-16 to 2016-03-24 along the reef flat with live coral cover. Seawater nutrients and carbonate chemistry variables were collected every 4 h during each sampling period from the primary vent site and in adjacent coastal waters along the shallow reef at Kahekili (Fig. 1). The first sampling period was from 15:00 on 2016-03-16 to 15:00 on 2016-03-19, and the second sampling period was from 15:00 on 2016-03-21 to 11:00 on 2016-03-24 (all reported times in local [HST]). There were five sampling sites: two shallow (<1.5 m) sites (S1 and S2) located approximately 10 m offshore, two deeper (5 m) sites (S3 and S4) located approximately 115 m offshore, and a shallow site located approximately 20 m offshore and within 0.25 m of an active SGD vent (vent site; <1.5 m) (Glenn et al., 2013;Swarzenski et al., 2016). Sampling tubes (ranging from approximately 100 to 200 m in length) were installed at each site by affixing the tube to a concrete block located approximately 20 cm above the seafloor, or by attaching the tubing directly to dead reef structure using zip ties. Tube intakes were fitted with a stainless steel screen cap to prevent uptake of large particulates. The remaining length of each tube was positioned along the seafloor to the adjacent beach by weighting the tube with a 1 m piece of chain, or by weaving the tube through dead reef structure approximately every 20 m. The tube outflow ends were labeled for each sampling site, bundled in a common location, and located above the high water line on the beach for sampling access. A peristaltic pump was used to pump seawater from the seafloor. Sampling tubes were flushed for a minimum of 20 minutes to remove residual seawater before collecting data and water samples. Sampling tubes were inspected upon extraction and no significant algal growth was observed. Temperature salinity, and dissolved oxygen of water samples were measured using a YSI ProPlus multimeter that was calibrated daily with an accuracy of ± 0.2°C, ± 0.1 psu, and ± 0.2 mg L^{-1}, respectively. However, due to temperature change during water transit time within the sampling tube, in situ temperatures were also recorded from Solonist CTD Divers installed at the intake of each sampling tube. An upward-looking 2-MHz Nortek Aquadopp acoustic Doppler profiler (ADP) was deployed at the southern deeper site (S4). The ADP sampled waves at 2 Hz for 17 min every hour and currents at 1 Hz every 10 min in 1-m vertical bins from 1 m above the seabed up to the ocean surface.

2.3 Seawater Analyses

Samples for dissolved nutrients (NH_4^+, Si, PO_4^{3-}, and [NO_3^-+NO_2^-]) were collected in duplicate by filtering water with an in-line 0.45-μm cellulose nitrate filter and 0.20-μm polyethersulfone syringe filter, and were kept frozen until analysis. Nutrients were analyzed at the Woods Hole Oceanographic Institution's nutrient laboratory and University of California at Santa Barbara's Marine Science

Institute Analytical Laboratory via flow injection analysis for NH_4^+, Si, PO_4^{3-}, and [NO_3^-+ NO_2^-], with precisions of 0.6-3.0%, 0.6-0.8%, 0.9-1.3%, and 0.3%-1.0% relative standard deviations, respectively. Select samples were collected and analyzed for nitrate isotope ($\delta^{15}N$ and $\delta^{18}O$) analyses at the University of California at Santa Cruz using the chemical reduction method (McIlvin and Altabet, 2005;Ryabenko et al., 2009) and University of California at Davis' Stable Isotope Facilities using the denitrifier method (Sigman et al., 2001). The isotope analysis was conducted using a Thermo Finnigan MAT 252 coupled with a GasBench II interface; isotope values are presented in per mil (‰) with respect to AIR for $\delta^{15}N$ and VSMO for $\delta^{18}O$ with a precision of 0.3-0.4‰ and 0.5-0.6‰ for $\delta^{15}N$-nitrate and $\delta^{18}O$-nitrate, respectively.

Seawater samples for determining carbonate chemistry variables (pH on the total scale, TA, and DIC) were collected from the 5 sampling sites using a peristaltic pump and pressure filtering seawater through a 0.45-μm filter. Samples for pH (0.007±0.017) were filtered into 30-mL optical glass cells and analyzed within 1 h of collection using spectrophotometric methods (Zhang and Byrne, 1996), an Ocean Optics USB2000 spectrometer, and thymol blue indicator dye. Samples for TA and DIC were filtered into 300-ml borosilicate glass bottles, preserved by adding 100 μL saturated $HgCl_2$ solution and pressure sealed with ground glass stoppers coated with Apiezon grease. TA samples were analyzed using spectrophotometric methods of Yao and Byrne (1998) with an Ocean Optics USB2000 spectrometer and bromocresol purple indicator dye. DIC samples were analyzed using a UIC carbon coulometer model CM5014 and CM5130 acidification module fitted with a sulfide scrubber, and methods of Dickson et al. (2007). In situ temperatures recorded from Solonist CTD Divers were reported and used to temperature-correct pH and perform CO2SYS calculations as described below.

Certified reference materials (CRM) for TA and DIC analyses were from the Marine Physical Laboratory of Scripps Institution of Oceanography (Dickson et al., 2007). TA and DIC sample accuracy were within 0.56 ±0.55 and 1.50 ± 1.17 μmol kg^{-1} of certified reference material respectively. Precision for TA based on replicate sample analyses was 0.76 ± 0.83 μmol kg^{-1}. Precision for DIC based on replicate sample analyses was 1.9 ± 1.5 μmol kg^{-1}. The full seawater CO_2 system was calculated with measured salinity, temperature, nutrients (phosphate and silicate), TA, DIC, and pH data using an Excel Workbook Macro translation of the original CO2SYS program (Pierrot et al., 2006). Given the enriched nutrient setting of the study site, TA values were nutrient corrected in CO2SYS (Dickson, 1981). The aragonite saturation state (Ω_{arag}) and pCO_2 are reported based on DIC-pH pairs, with dissociation constants K_1 and K_2 from Mehrbach et al. (1973) refit by Dickson and

Millero (1987) and KSO_4 from Dickson (1990). The TA and DIC values were normalized to salinity (by multiplying by a factor of 35/S, where S is the measured salinity value) to account for variations in TA and DIC along the reef flat driven by evaporation and/or precipitation (Friis et al., 2003) and are reported as *n*TA and *n*DIC as previously established in reef geochemical surveys (e.g., Suzuki and Kawahata, 2003; Yates et al., 2014; Muehllehner et al., 2016) where TA and DIC exhibit non-conservative behavior with respect to salinity. However at the vent site the TA and DIC data was not normalized to salinity given the contribution of TA and DIC from SGD.

2.4 Statistical Analysis

Slope of salinity normalized total alkalinity (*n*TA): salinity normalized dissolved inorganic carbon (DIC), net community calcification: net community production ratio (NCC:NCP=2ΔDIC/(ΔTA-1)) (Suzuki and Kawahata, 2003), correlation coefficients (r^2), analysis of variance (ANOVA), and standard error of difference (SE_{dif}) were calculated in Excel v. 14.7.6. Histogram plots and cubic spline fits were made in KaleidaGraph 4.1.3.

3. Results

3.1 Submarine Groundwater Endmember

The magnitude of change and absolute values in the carbonate chemistry, nutrients, and salinity were greatest at the primary vent site relative to the four sites along the reef. The salinity ranged from 10.64 to 36.72 over the 6-d period (Fig. 2A), with the most dramatic decrease in salinity on 2016-03-22 when salinity decreased from 32.45 to 12.47 within 4 h. The reduction in salinity was sustained over a 32-h period. A rapid change was also observed in the pH, DO, TA, DIC, and nutrient concentrations (Fig. 2). For example, nitrate concentrations at the vent site ranged from 0.45 to over 70 μmol L^{-1}, with an average nitrate concentration of 117 (SD 0.09) μmol L^{-1} measured directly from the discharging seep water. The Ω_{arag} values decreased to less than 1 and pCO_2 values increased to 2000 μatm when salinity values dropped to less than 15 (Fig. 2D). No diurnal pattern was detected in the seawater carbonate chemistry at this site. Instead, these results are consistent with earlier work documenting lower pH, nutrient enriched freshwater endmember values tightly coupled to SGD (Swarzenski et al., 2012; Glenn et al., 2013;Swarzenski et al., 2016).

3.2 Reef Flat

In contrast to the vent site, the overall magnitude of carbonate chemistry variation at the other four sites along the reef flat was less, and the signal was coherent among these sites. This coherency is

captured in the pH time series (Fig. 3B), where the pH data from the four sites were significantly (p<0.05) positively correlated with each other (with r ~ 0.5). The lowest salinity value along the reef flat was 33.51, indicating minimal freshwater influence on reef flat salinity. As a result, the carbonate system parameters measured along the reef were non-linear with respect to salinity (Supplemental Fig. 1), instead a diurnal pattern dominated the signal (Fig. 3). Lowest pH values occurred around midnight (23:00); and highest pH values occurred in the afternoon (~14:00-15:00). This diurnal pattern was also apparent in the DIC data, with lowest values in the afternoon and increasing around midnight, with a cubic spline fit (Press et al., 1988) highlighting diurnal cycle from all four sites along the reef flat. Likewise, the diurnal signal was identifiable in the Ω_{arag} and pCO_2 time-series, with Ω_{arag} values increasing and pCO_2 decreasing during the mid-day hours (Fig. 3). The diurnal signal in the nTA time-series was similar to the signal for nDIC. At the shallow (<5 m) sites, pH and DO covaried (r^2=0.43-0.87; p<0.001). The range in pH and Ω_{arag} was largest at the shallow sites; however, the average values were similar along the reef, 3.02 to 3.06 and 8.00 to 8.01, respectively, and were elevated relative to the average values recorded at the vent site, 7.85 (SD 0.17) and 2.28 (SD 0.81) for pH and Ω_{arag}, respectively (Prouty et al., 2017b). No diurnal pattern was observed for the nutrient data; however, there was an offshore gradient in nutrient concentrations with enriched nutrients at the shallow sites compared to the deeper sites. Nutrient concentrations (Si, PO_4^{3-}, and NO_3^-) from the two shallow sites were statistically greater than the two deeper sites according to pairwise multi-comparison one-way ANOVA with a *post hoc* Tukey HSD (p>0.05). For example average nitrate concentrations at the two shallow sites were 0.71 (SD 0.35) and 0.41 (0.18 SD) compared to 0.17 (SD 0.10) and 0.19 (SD 0.11) μmol L^{-1}. Deficits and surpluses of nTA and nDIC, with respect to open ocean conditions, were calculated as ΔnTA and ΔnDIC using values from Station HOT (Dore et al., 2009), located approximately 250 km offshore as reported from 1988 to 2015 (http://hahana.soest.hawaii.edu/hot/products/products.html). The ΔnTA values ranged from -332 μmol kg^{-1} to 85 μmol kg^{-1} and -171 μmol kg^{-1} to 141 μmol kg^{-1} ΔnDIC. The standard error of difference (SE_{dif}) was calculated for ΔnTA and ΔnDIC values to evaluate whether the deficits and surpluses of nTA and nDIC were significant. Histogram plots reveal statistical (p=0.05; critical t value of 1.68; df=37) deficits and surpluses as well as differences between the first and second half of the sampling period (Fig. 4). Results show a shift from a deficit in ΔnTA to a surplus in ΔnTA at all stations, as well as a shift from a deficit in ΔnDIC to a surplus in ΔnDIC, suggesting a shift in the second sampling period from $CaCO_3$ production to $CaCO_3$ dissolution, and from photosynthesis to respiration. This change was most distinct at the two shallow sites. The nTA and nDIC values from the second sampling period were also enriched relative to a range of values reported from nearshore Oahu sites (Drupp et

al., 2013) but consistent with coastal sites from Maunalau Bay, Oahu with known inputs of SGD (Nelson et al., 2015; Richardson et al., 2017).

4. Discussion

The diurnal pattern observed at the four sampling sites along the reef flat is typical of a reef environment where biotic processes involving coral reef community metabolism (e.g., respiration/photosynthesis and calcification/dissolution) dominate the carbonate chemistry system (e.g., Smith, 1973). The non-linear relationship between salinity and carbonate chemistry parameters further supports the notion that biotic processes are driving carbonate chemistry variability along the reef flat (Millero et al., 1998; Ianson et al., 2003). The lower amplitude *n*TA diurnal signal supports previous observations that the region was algal-dominated (Smith et al., 2005). In this case, the lower biomass of calcifying organisms leads to conditions that favor respiration-photosynthesis processes relative to calcification-dissolution (Jokiel et al., 2014). Elevated pH values during mid-day, coincident with elevated sea surface temperature (SST) and peak solar irradiance, are consistent with maximum photosynthetic activity. DIC decreased during the day due to photosynthesis, whereas at nighttime, pH decreased and DIC increased in response to respiration (Fig. 3). This pattern is in stark contrast to the primary vent site where no diurnal pattern was observed, and abiotic controls on the carbonate system dynamics explain the strong linear relation to salinity. Variability at the vent site is driven by SGD rates, which are elevated during low tide when hydraulic gradients are the steepest (Dimova et al., 2012;Swarzenski et al., 2016). This spatial pattern is consistent with offshore transects from Maunalua Bay where sites closest to shore incorporated greater contribution of SGD derived TA and DIC than offshore sites (Richardson et al., 2017).

To further understand the temporal variability in carbonate chemistry over the 6-d sampling period along the reef flat, diagrams of *n*TA versus *n*DIC were plotted according to Zeebe and Wolf-Gladrow, (2001), along with vectors indicating theoretical effects of net community production (NCP) and net community calcification (NCC) on seawater chemistry (Kawahata et al., 1997;Suzuki and Kawahata, 2003) (Fig 5). As presented here, NCP refers to the balance of photosynthesis and respiration, and NCC refers to the balance between calcification and dissolution (see review by Cyronak et al., 2018). Diagrams of *n*TA-*n*DIC indicate the dominance of photosynthesis (+NCP) and $CaCO_3$ precipitation (+NCC) during the first sampling period (2016-03-16 to 2016-03-19). The slope values of the *n*DIC-*n*TA plots were used to calculate ratios of NCC:NCP (Table 1) using methods of Suzuki and Kawahata (2003) to estimate the relative contribution of these processes to reef biogeochemistry. In the absence

of reliable water mass residence time, ratios were used rather than metabolic rates. The NCC:NCP ratios for the first sampling period ranged from 0.50 to 0.87 indicating a dominance of NCP relative to NCC. Plots of *n*DIC-*n*TA (Fig. 5) indicate that these sites were dominated primary by photosynthesis and calcification during +NCP and +NCC. This pattern was observed at all four sites along the reef flat. The lower NCC:NCP ratios at the shallow sites highlight the greater vulnerability of the shallow sites to dissolution under lower pH conditions relative to the deeper. These results are in agreement with Richardson et al. (2017) that found dissolution at reef sites closet to groundwater vents in Maunalua Bay, Oahu. A shift occurred at all sampling sites after the first sampling period. Elevated *n*DIC and *n*TA values from 2016-03-21 to 2016-03-22 indicate a shift to respiration and dissolution in the *n*TA-*n*DIC diagrams during –NCC and –NCP (Fig. 5). At the shallow sites, S1 and S2 (Fig. 5A and B), the NCC:NCP ratios were 0.56 and 0.39 during the second sampling period (Table 1), respectively, indicating the dominance of NCP relative to NCC. In comparison, at sites S3 and S4 located further offshore, dissolution and respiration contributed nearly equally with NCC:NCP ratios near 1.0 during the second sampling. Given the salinity range along the reef flat (34 to 36), traditional salinity normalization (e.g., Friis et al., 2003) could potentially overestimate the *n*DIC and *n*TA concentrations by ~20 to ~10 μmol kg^{-1} respectively, according to non-zero normalization described in Richardson et al. (2017). However, rather than reflecting an artifact of the salinity normalization, given the non-linear relation of DIC and TA to salinity along the reef flat (Fig. S1), this shift is interpreted as a reef community response. As shown in Figures 4 and 5, this change captures a shift from a reef community dominated by calcification and photosynthesis to one dominated by respiration and dissolution during –NCC and -NCP.

The shift from photosynthesis (P) to respiration (R) as captured in the Δ*n*DIC histogram plots (Fig. 4), suggests that the coral-algal association consumed more energy than it produced during the second sampling period. As a proxy for autotrophic capacity, the change in P:R ratio may reflect an increase in coral heterotrophic feeding relative to autotrophic feeding (Coles and Jokiel, 1977;Hughes and Grottoli, 2013). Typically, stored lipid reserves in the tissue are utilized when the stable symbiotic environment is disturbed (e.g., Szmant and Gassman, 1990; Ainsworth et al., 2008). Although short-lived, thermally-induced bleaching has been linked to depletion of coral lipid reserves (e.g., Hughes and Grottoli, 2013), excess nutrient loading can also shift the stability of the coral-algae symbiosis, thereby reducing stored tissue reserves (Wooldridge, 2016). According to Glenn et al. (2013), up to 11 m^3 d^{-1} of dissolved inorganic nitrogen are discharged onto the West Maui reef as the result of receiving and treating over 15,000 m^3 d^{-1} of sewage. Using a SGD flux rate of 87 cm d^{-1} at the primary seep site

(Swarzenski et al., 2016), and SGD nitrate end-member concentration of 117 μmol L^{-1} (Prouty et al., 2017b), the nitrate flux from the primary vent site is 712 mol d^{-1}, clearly demonstrating excess nutrient loading. Elevated SGD end-member nutrient concentrations are consistent with those observed from Black Point, Maunalua Bay where effluent from proximal on-site sewage disposal is linked to excess nitrogen loads (Nelson et al., 2015; Richardson et al., 2017). As described above, an offshore gradient in nutrient concentrations was observed with enriched nutrients at the shallow sites compared to the deeper sites, consistent with a decrease in coral $\delta^{15}N$ values away from the vent (Prouty et al., 2017a). Coral tissue thickness was also negatively correlated to coral tissue $\delta^{15}N$ values (r = -0.66; p = 0.08), with the latter serving as a proxy for nutrient loading in alga samples along the reef flat (Dailer et al., 2010). It is possible that a reduction in coral tissue reflects preferential heterotrophic feeding under high nutrient loading, with nutrient enrichment by sewage effluent increasing primary production and biomass in the water column (e.g., Smith et al., 1981; Pastorok and Bilyard, 1985). While assessing the impacts of nutrient loading on coral physiology may be long term and subtle in some cases, results from our study highlight the potential short-term impacts of nutrification.

Identifying the exact mechanism(s) responsible for driving this shift is difficult given the complexity of the reef system. Possible explanations include warmer SSTs, suspension of organic matter, as well as secondary effects of nutrification from contaminated SGD (D'Angelo and Wiedenmann, 2014). Given that microbial communities rapidly take up inorganic nutrients (Furnas et al., 2005), there could be increased respiration as a result of increased microbial remineralization of organic matter in the nutrient-loaded environment (Sunda and Cai 2012). In other words, enhanced SGD-driven nutrient fluxes during the second sampling period could have increased microbial growth and remineralization, shifting the reef community metabolism, as captured in a shift in the carbonate chemistry system. In addition to community metabolism, local oceanographic effects such as the wind and wave regime can also drive carbonate chemistry by altering air-sea exchange and water mass residence times. During the first sampling period, the wave height increased from 0.4 m to 1.6 m over the first 2 d and mean current speeds were 1.6 cm s^{-1} (Fig. S2). In comparison, during the second sampling period, wave height declined to less than 0.4 m and mean current speeds were 1.0 cm s^{-1}. Together, the reduced wave height and reduced wind speeds favor slower release of CO_2 generated by calcification and respiration processes from the water column (Massaro et al., 2012), resulting in higher pCO_2 and lower pH.

Despite being situated in an oligotrophic region with naturally occurring, low nutrient concentrations,

anthropogenic nutrient loading to coastal waters via sustained SGD is driving nearshore eutrophication (Dailer et al., 2010; Dailer et al., 2012; Bishop et al., 2015; Amato et al., 2016; Fackrell et al., 2016), with algal $\delta^{15}N$ signatures at Kahekili Beach Park indicative of wastewater effluent (Dailer et al., 2010;Dailer et al., 2012). In response, there has been a shift in benthic cover from abundant corals to turf- or macro-algae over the last two decades. Areas of discrete coral cover loss up to 100% along the shallow coral reef at Kahekili have been observed for decades (Wiltse, 1996; Ross et al., 2012), with a history of macro-algal blooms (Smith et al., 2005). More recently, Prouty et al. (2017a) found accelerated nutrient driven-bioerosion from coral cores collected along the Kahekili reef flat in response to land-based sources of nutrients. This is consistent with earlier work showing nutrification-mediated increase in plankton loads can trigger increases in filter feeders and bioeroders that endanger reef structure integrity (e.g., Fabricius et al., 2012). Eutrophication from nutrient enriched SGD may contribute to an already compromised carbonate system (i.e., reduced pH and Ω_{arag}) by increasing respiration and remineralization of excess organic matter, and increasing bioerosion. Therefore, secondary effects of nutrient-driven increase in phytoplankton biomass and decomposing organic matter are also important considerations for coral reef management (D'Angelo and Wiedenmann, 2014).

As discussed above, SGD rates are elevated during low tide when the relative pressure head between terrestrial groundwater and the oceanic water column is greatest (Dimova et al., 2012;Swarzenski et al., 2016). Relative SGD is greater in the shallows close to shore where the tidal height is larger relative to the depth of the water column. Higher islands, therefore, have the potential for not only greater orographic rainfall and thus submarine groundwater recharge, but also greater potential pressure head and thus enhanced SGD- driven nutrient fluxes. There is also greater potential for enriched nutrient sources and reduced water quality with fast-growing population and development (Amato et al., 2016;Fackrell et al., 2016). Thus, SGD represents a key vector of nutrient loading in tropical, oligotrophic regions (e.g., Paytan et al., 2006). At the same time, closer to shore, current speeds are generally slower resulting in longer water mass residence times (Storlazzi et al., 2006); longer residence times would also be expected closer to the seabed, compared with upper water column flows (Storlazzi and Jaffe, 2008). Together, these suggest that the resulting exposure (= intensity x residence time) of coral reefs to nutrient-laden, low pH submarine groundwater is greater for coral reefs closer to shore off high islands than along barrier reefs or on atolls. This heightened vulnerability therefore needs to be taken into account when evaluating vulnerability of nearshore fringing reefs to changes in carbonate chemistry system given evidence of nutrient driven-bioerosion

from land-based sources of pollution.

5. Conclusion

Field based measurements of carbonate chemistry variability were made along a shallow coral reef off Kahekili, west Maui, and captured differences in the relative importance of inorganic and organic carbon production over a 6-d period in March 2016. Submarine groundwater discharge fluxes controlled the carbonate chemistry adjacent to the primary vent site, with nutrient-laden freshwater decreasing the pH levels and favoring undersaturated Ω_{arag} conditions. In contrast, reef community metabolism dominated the carbonate chemistry diurnal signal at sites along the reef flat. Superimposed on the diurnal signal was a transition during the second sampling period, yielding a surplus of *n*TA and *n*DIC compared to ocean endmember measurements indicating a shift from photosynthesis and calcification during +NCP and + NCC to respiration and carbonate dissolution during –NCC and -NCP. This shift could be interpreted as a direct response to increased nutrient loading, and subsequent enhancement of organic matter remineralization. Predictions of reef response to elevated pCO_2 levels assume reef water tracks open-ocean pH, however local effects are equally important (e.g., Cyronak et al., 2013; 2018), particularly along densely-inhabited shorelines with known input from land-based sources of pollution. Building on previous work documenting the input of nutrient laden, low-pH freshwater to the reefs off Kahekili, results presented here offer a first glimpse into how anthropogenic-driven eutrophication might add an additional stressor to thresholds tipping the balance between net carbonate accretion and net carbonate dissolution, thus altering carbonate system dynamics.

Author contribution

NGP and KKY designed the experiments and NGP, KKY, NS and CG carried them out. NGP and KKY completed the chemical measurements and OC compiled the oceanographic data. NGP prepared the manuscript with contributions from all co-authors.

The authors declare that they have no conflict of interest.

Acknowledgements

This research was carried out as part of the US Geological Survey's Coral Reefs Project in an effort to better understand the effects of geologic and oceanographic processes on coral reef systems in the USA and its trust territories, and was supported by the USGS Coastal and Marine Geology Program. The authors gratefully acknowledge the vital partnership and expert logistics support provided by the State of Hawaii Division of Aquatic Resources. We thank T. DeCarlo (UWA), H. Barkley (NOAA),

two anonymous reviewers, and J.P. Gattuso for their valuable reviews, A. Cohen (WHOI) for helpful discussions, and K.R. Pietro and K. Hoering (WHOI), C. Moore (USGS), and G. Paradis (UCSB) analytical assistance, M. Dailer (U. Hawaii) for field assistance. The use of trade names is for descriptive purposes only and does not imply endorsement by the U.S. Government. Additional data to support this project can be found in Prouty et al., (2017b).

Figure Captions

Figure 1. Location map of the island of Maui, Hawaii, USA, and the study area along west Maui. Bathymetric map (5-m contours) of study area showing seawater sampling locations (blue closed circle) along Kahekili Beach Park, and the primary seep site (blue open circle) superimposed on distribution of percent coral cover versus sand.

Figure 2 Results of time-series of seawater chemistry variables over a 6-d period collected from the seep site located on the nearshore reef every 4 h. (A) Salinity, (B) dissolved nutrient (nitrate+nitrite, phosphate, and silicate) concentrations (μmol L^{-1}), and nitrate stable nitrogen isotopes (δ^{15}N-nitrate; ‰), (C) total alkalinity (TA) and dissolved inorganic carbon (DIC) (μmol kg^{-1}), (D) calculated carbonate parameters for aragonite saturation state (Ω_{arag}), and pCO_2 (μatm; inverted) based on DIC-pH pairwise and measured salinity, temperature, nutrients (phosphate and silicate) data, (E) dissolved oxygen (DO; mg L^{-1}), and (F) temperature corrected pH (total scale). End-of-century projections according to IPCC-AR5 RCP8.5 "business as usual" scenario for pH (reduction by 0.4 units), Ω_{arag} (2.0; blue dashed), and pCO_2 (750 μatm; red dashed).

Figure 3 Carbonate chemistry parameters and sea surface temperature (SST) composite from S1, S2, S3 and S4 along the shallow reef flat of Kahekili, Maui and cubic spline fits highlighting diurnal cycle for the first (2016-03-16 to 2016-03-19; solid line) and second (2016-03-21 to 2016-03-24; dashed line) sampling period for (A) Temperature, (B) pH, (C) *n*DIC and (D) *n*TA (μmol kg^{-1}), (E) Ω_{arag} and (F) pCO_2 (μatm).

Figure 4 Histogram Δ*n*TA and Δ*n*DIC capturing deficits and surpluses of *n*TA and *n*DIC with respect to open ocean conditions. Overall a transition from $CaCO_3$ production to $CaCO_3$ dissolution and photosynthesis to respiration occurred between the first (2016-03-16 to 2016-03-19; blue) and second (2016-03-21 to 2016-03-24; red) sampling period for the shallow sampling sites (A)-(B) S1 and (C)-

(D) S2, and the two deeper sites (E)-(F) S3, and (G-H) S4. Statistical (p=0.05) deficit and surplus values (±) for ΔnTA and ΔnTA shown in parentheses.

Figure 5 Seawater carbonate chemistry system along the reef flat off Kahekili as a function of nDIC and nTA for the shallow sampling sites (A). S1 and (B) S2, and two deeper sites (C) S3, and (D) S4 for the first (blue) and second (red) sampling periods and their respective slopes (solid lines) of nDIC and nTA (Table 1) and theoretical slope (dashed lines) given the predicted net effects of photosynthesis, respiration, calcification, and dissolution as shown in (E) and the respective change in net community calcification (NCC) and net community production (NCP). The relative position of the open ocean nDIC and nDIC values are reported as 1977 (SD 11) and 2304 (SD 5) μmol kg^{-1} (adapted from Dore et al., 2009).

References

Ainsworth, T. D., Hoegh-Guldberg, O., Heron, S. F., Skirving, W. J., and Leggat, W.: Early cellular changes are indicators of pre-bleaching thermal stress in the coral host, J Exp Mar Biol Ecol, 364, 63-71, 10.1016/j.jembe.2008.06.032, 2008.

Albright, R., Benthuysen, J., Cantin, N., Caldeira, K., and Anthony, K.: Coral reef metabolism and carbon chemistry dynamics of a coral reef flat, Geophys Res Lett, 42, 3980-3988, 10.1002/2015GL063488, 2015.

Amato, D. W., Bishop, J. M., Glenn, C. R., Dulai, H., and Smith, C. M.: Impact of submarine groundwater discharge on marine water quality and reef biota of Maui, PloS one, 11, e0165825, 10.1371/journal.pone.0165825 2016.

Anderson, D. M., Glibert, P. M., and Burkholder, J. M.: Harmful algal blooms and eutrophication: nutrient sources, composition and consequences., Estuaries, 25, 562–584., 10.1007/BF02804901, 2002.

Andersson, A. J., and Gledhill, D.: Ocean acidification and coral reefs: effects on breakdown, dissolution, and net ecosystem calcification, Annual Review of Marine Science, 5, 321-348, 2013.

Andrefouet, S., Mumby, P. J., McField, M., Hu, C., and Muller-Karger, F. E.: Revisiting coral reef connectivity, Coral Reefs, 21, 43-48, 10.1007/s00338-001-0199-0, 2002.

Bernstein, W. N., Hughen, K. A., Langdon, C., McCorkle, D. C., and Lentz, S. J.: Environmental controls on daytime net community calcification on a Red Sea reef flat, Coral Reefs, 35, 697-711, 2016.

Bishop, J. M., Glenn, C. R., Amato, D. W., and Dulai, H.: Effect of land use and groundwater flow path on submarine groundwater discharge nutrient flux, Journal of Hydrology: Regional Studies, 10.1016/j.ejrh.2015.10.008, 2015.

Cai, W.-J., Hu, X., Huang, W.-J., Murrell, M. C., Lehrter, J. C., Lohrenz, S. E., Chou, W.-C., Zhai, W., Hollibaugh, J. T., Wang, Y., Zhao, P., Guo, X., Gundersen, K., Dai, M., and Gong, G.-C.: Acidification of subsurface coastal waters enhanced by eutrophication, Nature Geoscience, 4, 766, 10.1038/ngeo1297, 2011.

Cochran, S. A., Gibbs, A. E., and D.J., W.: Benthic habitat map of the U.S. Coral Reef Task Force Watershed Partnership Initiative Kā‘anapali priority study area and the State of Hawai‘i

Kahekili Herbivore Fisheries Management Area, west-central Maui, Hawai‘i, p. 42 p., U.S. Geological Survey Open-File Report 2014-1129, 2014.
Coles, S. L., and Jokiel, P. L.: Effects of temperature on photosynthesis and respiration in hermatypic corals, Mar Biol, 43, 209-216, 10.1007/BF00402313, 1977.
Cyronak, T., Santos, I. R., and Eyre, B. D.: Permeable coral reef sediment dissolution driven by elevated pCO_2 and pore water advection, Geophys Res Lett, 40, 4876-4881, 10.1002/grl.50948, 2013.
Cyronak, T., Andersson, A. J., Langdon, C., Albright, R., Bates, N. R., Caldeira, K., Carlton, R., Corredor, J. E., Dunbar, R. B., Enochs, I., Erez, J., Eyre, B. D., Gattuso, J.-P., Gledhill, D., Kayanne, H., Kline, D. I., Koweek, D. A., Lantz, C., Lazar, B., Manzello, D., McMahon, A., Meléndez, M., Page, H. N., Santos, I. R., Schulz, K. G., Shaw, E., Silverman, J., Suzuki, A., Teneva, L., Watanabe, A., and Yamamoto, S.: Taking the metabolic pulse of the world's coral reefs, PLOS ONE, 13, e0190872, 10.1371/journal.pone.0190872, 2018.
D'Angelo, C., and Wiedenmann, J.: Impacts of nutrient enrichment on coral reefs: new perspectives and implications for coastal management and reef survival, Current Opinion in Environmental Sustainability, 7, 82-93, doi.org/10.1016/j.cosust.2013.11.029, 2014.
Dailer, M. L., Knox, R. S., Smith, J. E., Napier, M., and Smith, C. M.: Using $\delta^{15}N$ values in algal tissue to map locations and potential sources of anthropogenic nutrient inputs on the island of Maui, Hawai‘i, USA, Mar Pollut Bull, 60, 655-671, 10.1016/j.marpolbul.2009.12.021, 2010.
Dailer, M. L., Ramey, H. L., Saephan, S., and Smith, C. M.: Algal $\delta^{15}N$ values detect a wastewater effluent plume in nearshore and offshore surface waters and three-dimensionally model the plume across a coral reef on Maui, Hawai‘i, USA, Mar Pollut Bull, 64, 207-213, 10.1016/j.marpolbul.2011.12.004, 2012.
DeCarlo, T. M., Cohen, A. L., Wong, G. T. F., Shiah, F. K., Lentz, S. J., Davis, K. A., Shamberger, K. E. F., and Lohmann, P.: Community production modulates coral reef pH and the sensitivity of ecosystem calcification to ocean acidification, Journal of Geophysical Research: Oceans, 122, 2017.
Dickson, A. G.: An exact definition of total alkalinity and a procedure for the estimation of alkalinity and total inorganic carbon from titration data, Deep-Sea Res, 28A, 609-623, 1981.
Dickson, A. G.: Thermodynamics of the dissociation of boric acid in synthetic seawater from 273.15 to 318.15 K, Deep Sea Research Part A. Oceanographic Research Papers, 37, 755-766, 10.1016/0198-0149(90)90004-F, 1990.
Dickson, A. G., and Millero, F. J.: A comparison of the equilibrium constants for the dissociation of carbonic acid in seawater media, Deep Sea Research Part A. Oceanographic Research Papers, 34, 1733-1743, 10.1016/0198-0149(87)90021-5, 1987.
Dickson, A. G., Sabine, C. L., and Christian, J. R.: Guide to best practices for ocean CO_2 measurements, PICES Special Publication, 3, 176, 2007.
Dimova, N. T., Swarzenski, P. W., Dulaiova, H., and Glenn, C. R.: Utilizing multichannel electrical resistivity methods to examine the dynamics of the fresh water–seawater interface in two Hawaiian groundwater systems, Journal of Geophysical Research: Oceans, 117, 10.1029/2011jc007509, 2012.
Dore, J. E., Lukas, R., Sadler, D. W., Church, M. J., and Karl, D. M.: Physical and biogeochemical modulation of ocean acidification in the central North Pacific, Proceedings of the National Academy of Sciences, 106, 12235-12240, 2009.
Drupp, P. S., De Carlo, E. H., Mackenzie, F. T., Sabine, C. L., Feely, R. A., and Shamberger, K. E.: Comparison of CO_2 dynamics and air–sea gas exchange in differing tropical reef environments, Aquat Geochem, 19, 371-397, 2013.
Fabricius, K. E.: Effects of terrestrial runoff on the ecology of corals and coral reefs: review and synthesis, Mar Poll Bull, 50, 125-146, 10.1016/j.marpolbul.2004.11.028, 2005.

Fabricius, K. E., Cooper, T. F., Humphrey, C., Uthicke, S., De'ath, G., Davidson, J., LeGrand, H., Thompson, A., and Schaffelke, B.: A bioindicator system for water quality on inshore coral reefs of the Great Barrier Reef, Mar Pollut Bull, 65, 320-332, doi.org/10.1016/j.marpolbul.2011.09.004, 2012.

Fackrell, J. K., Glenn, C. R., Popp, B. N., Whittier, R. B., and Dulai, H.: Wastewater injection, aquifer biogeochemical reactions, and resultant groundwater N fluxes to coastal waters: Kā'anapali, Maui, Hawai'i, Mar Pollut Bull, 110, 281-292, 10.1016/j.marpolbul.2016.06.050, 2016.

Ferrario, F., Beck, M. W., Storlazzi, C. D., Micheli, F., Shepard, C. C., and Airoldi, L.: The effectiveness of coral reefs for coastal hazard risk reduction and adaptation, Nature Communications, 5, 10.1038/ncomms4794, 2014.

Friis, K., Körtzinger, A., and Wallace, D. W. R.: The salinity normalization of marine inorganic carbon chemistry data, Geophys Res Lett, 30, 2003.

Furnas, M., Mitchell, A., Skuza, M., and Brodie, J.: In the other 90%: phytoplankton responses to enhanced nutrient availability in the Great Barrier Reef Lagoon, Mar Pollut Bull, 51, 253-265, 10.1016/j.marpolbul.2004.11.010, 2005.

Giambelluca, T. W., Chen, Q., Frazier, A. G., Price, J. P., Chen, Y.-L., Chu, P.-S., Eischeid, J. K., and Delparte, D. M.: Online Rainfall Atlas of Hawai'i, Bull. Amer. Meteor. Soc., 94, 313-316, 10.1175/BAMS-D-11-00228.1., 2013.

Glenn, C. R., Whittier, R. B., Dailer, M. L., Dulaiova, H., El-Kadi, A. I., Fackrell, J., Kelly, J. L., Waters, C. A., and Sevadjian, L.: Lahaina Groundwater Tracer Study – Lahaina,Maui, Hawaii, Final Report, p. 502 p., State of Hawaii Department of Health, the U.S. Environmental Protection Agency, and the U.S. Army Engineer Research and Development Center, 2013.

Howarth, R., Anderson, D., Cloern, J., Elfring, C., Hopkinson, C., Lapointe, B., Malone, T., Marcus, N., McGlathery, K., Sharpley, A., and Walker, D.: Nutrient pollution of coastal rivers, bays, and seas., Issues Ecol, 1 – 15, 2000.

Hughes, A. D., and Grottoli, A. G.: Heterotrophic compensation: A possible mechanism for resilience of coral reefs to global warming or a sign of prolonged stress?, PLOS ONE, 8, e81172, 10.1371/journal.pone.0081172, 2013.

Hughes, T. P., Baird, A. H., Bellwood, D. R., Card, M., Connolly, S. R., Folke, C., Grosberg, R., Hoegh-Guldberg, O., Jackson, J. B. C., Kleypas, J., Lough, J. M., Marshall, P., Nystrom, M., Palumbi, S. R., Pandolfi, J. M., Rosen, B., and Roughgarden, J.: Climate change, human impacts, and the resilience of coral reefs, Science, 301, 929-933, 10.1126/science.1085046, 2003.

Hughes, T. P., Rodrigues, M. J., Bellwood, D. R., Ceccarelli, D., Hoegh-Guldberg, O., McCook, L., Moltschaniwskyj, N., Pratchett, M. S., Steneck, R. S., and Willis, B.: Phase shifts, serbivory, and the resilience of coral reefs to climate change, Curr Biol, 17, 360-365, 10.1016/j.cub.2006.12.049, 2007.

Ianson, D., Allen, S. E., Harris, S. L., Orians, K. J., Varela, D. E., and Wong, C. S.: The inorganic carbon system in the coastal upwelling region west of Vancouver Island, Canada, Deep Sea Research Part I: Oceanographic Research Papers, 50, 1023-1042, 10.1016/S0967-0637(03)00114-6, 2003.

Jokiel, P. L., Jury, C. P., and Ku'ulei, S. R.: Coral-algae metabolism and diurnal changes in the CO_2-carbonate system of bulk sea water, PeerJ, 2, e378, 2014.

Kawahata, H., Suzuki, A., and Goto, K.: Coral reef ecosystems as a source of atmospheric CO_2: evidence from pCO_2 measurements of surface waters, Coral Reefs, 16, 261-266, 10.1007/s003380050082, 1997.

Knowlton, N., and Jackson, J. B. C.: Shifting baselines, local impacts, and global change on coral reefs, PLoS Biol, 6, e54, 2008.

Lantz, C. A., Atkinson, M. J., Winn, C. W., and Kahng, S. E.: Dissolved inorganic carbon and total alkalinity of a Hawaiian fringing reef: chemical techniques for monitoring the effects of ocean acidification on coral reefs, Coral Reefs, 33, 105-115, 2014.

Lapointe, B. E., Barile, P. J., Littler, M. M., and Littler, D. S.: Macroalgal blooms on southeast Florida coral reefs. II. Cross-shelf $\delta^{15}N$ values provide evidence of widespread sewage enrichment., Harmful Algae, 4, 1106–1122., 10.1016/j.hal.2005.06.004, 2005.

Massaro, R. F. S., De Carlo, E. H., Drupp, P. S., Mackenzie, F. T., Jones, S. M., Shamberger, K. E., Sabine, C. L., and Feely, R. A.: Multiple factors driving variability of CO_2 exchange between the ocean and atmosphere in a tropical coral reef environment, Aquat Geochem, 18, 357-386, 2012.

McIlvin, M. R., and Altabet, M. A.: Chemical conversion of nitrate and nitrite to nitrous oxide for nitrogen and oxygen isotopic analysis in freshwater and seawater, Anal Chem, 77, 5589-5595, 10.1021/ac050528s, 2005.

McMahon, A., Santos, I. R., Cyronak, T., and Eyre, B. D.: Hysteresis between coral reef calcification and the seawater aragonite saturation state, Geophys Res Lett, 40, 4675-4679, 10.1002/grl.50802, 2013.

Mehrbach, C., Culberson, C. H., Hawley, J. E., and Pytkowicx, R. M.: Measurement of the apparent dissociation constants of carbonic acid in seawater at atmospheric pressure, Limnol Oceanogr, 18, 897-907, 10.4319/lo.1973.18.6.0897, 1973.

Millero, F. J., Lee, K., and Roche, M.: Distribution of alkalinity in the surface waters of the major oceans, Mar Chem, 60, 111-130, 10.1016/S0304-4203(97)00084-4, 1998.

Muehllehner, N., Langdon, C., Venti, A., and Kadko, D.: Dynamics of carbonate chemistry, production, and calcification of the Florida Reef Tract (2009–2010): Evidence for seasonal dissolution, Global Biogeochem Cycles, 30, 661-688, 10.1002/2015GB005327, 2016.

Nelson, C. E., Donahue, M. J., Dulaiova, H., Goldberg, S. J., La Valle, F. F., Lubarsky, K., Miyano, J., Richardson, C., Silbiger, N. J., and Thomas, F. I. M.: Fluorescent dissolved organic matter as a multivariate biogeochemical tracer of submarine groundwater discharge in coral reef ecosystems, Mar Chem, 177, 232-243, doi.org/10.1016/j.marchem.2015.06.026, 2015.

Orr, J. C., Fabry, V. J., Aumont, O., Bopp, L., Doney, S. C., Feely, R. A., Gnanadesikan, A., Gruber, N., Ishida, A., Joos, F., Key, R. M., Lindsay, K., Maier-Reimer, E., Matear, R., Monfray, P., Mouchet, A., Najjar, R. G., Plattner, G.-K., Rodgers, K. B., Sabine, C. L., Sarmiento, J. L., Schlitzer, R., Slater, R. D., Totterdell, I. J., Weirig, M.-F., Yamanaka, Y., and Yool, A.: Anthropogenic ocean acidification over the twenty-first century and its impact on calcifying organisms, Nature, 437, 681-686, 2005.

Page, H. N., Courtney, T. A., Collins, A., De Carlo, E. H., and Andersson, A. J.: Net Community Metabolism and Seawater Carbonate Chemistry Scale Non-intuitively with Coral Cover, Frontiers in Marine Science, 4, 161, 2017.

Pastorok, R. A., and Bilyard, G. R.: Effects of sewage pollution on coral-reef communities, Mar Ecol Prog Ser, 175-189, 1985.

Paytan, A., Shellenbarger, G. G., Street, J. H., Gonneea, M. E., Davis, K., Young, M. B., and Moore, W. S.: Submarine groundwater discharge: An important source of new inorganic nitrogen to coral reef ecosystems, Limnol Oceanogr, 51, 343-348, 10.4319/lo.2006.51.1.0343, 2006.

Pierrot, D., Lewis, E., and Wallace, D. W. R.: MS Excel program developed for CO_2 system calculations, 2006.

Press, W. H., Flannery, B. P., Teukolsky, S. A., and Vetterling, W. T.: Numerical Recipes in C, Cambridge University Press, New York, 1988.

Prouty, N. G., Cohen, A., Yates, K. K., Storlazzi, C. D., Swarzenski, P. W., and White, D.: Vulnerability of Coral Reefs to Bioerosion From Land-Based Sources of Pollution, Journal of Geophysical Research: Oceans, 122, 9319-9331, 10.1002/2017JC013264, 2017a.

Prouty, N.G., Yates, K.K., Smiley, N.A., and Gallagher, C. Coral growth parameters and seawater chemistry, Kahekili, west Maui: U.S. Geological Survey data release, 10.5066/F7X34VPV, 2017b.
Richardson, C. M., Dulai, H., Popp, B. N., Ruttenberg, K., and Fackrell, J. K.: Submarine groundwater discharge drives biogeochemistry in two Hawaiian reefs, Limnol Oceanogr, 62, S348-S363, 10.1002/lno.10654, 2017.
Rodgers, K. u. S., Jokiel, P. L., Brown, E. K., Hau, S., and Sparks, R.: Over a decade of change in spatial and temporal dynamics of Hawaiian coral reef communities 1, Pac Sci, 69, 1-13, 10.2984/69.1.1, 2015.
Ross, M., White, D., Aiwohi, M., Walton, M., Sudek, M., Lager, D., and Jokiel, P.: Characterization of "dead zones" and population demography of Porites compressa along a gradient of anthropogenic nutrient input at Kahekili Beach Park, Maui, State of Hawaii, Department of Land and Natural Resources, Division of Aquatic Resources, Honolulu, Hawaii 96813, 2012.
Ryabenko, E., Altabet, M. A., and Wallace, D. W. R.: Effect of chloride on the chemical conversion of nitrate to nitrous oxide for $\delta^{15}N$ analysis, Limnol Oceanogr, Methods 7, 545-552, 10.4319/lom.2009.7.545, 2009.
Shamberger, K. E. F., Feely, R. A., Sabine, C. L., Atkinson, M. J., DeCarlo, E. H., Mackenzie, F. T., Drupp, P. S., and Butterfield, D. A.: Calcification and organic production on a Hawaiian coral reef, Mar Chem, 127, 64-75, 2011.
Shaw, E. C., McNeil, B. I., and Tilbrook, B.: Impacts of ocean acidification in naturally variable coral reef flat ecosystems, Journal of Geophysical Research: Oceans, 117, 2012.
Sigman, D. M., Casciotti, K. L., Andreani, M., Barford, C., Galanter, M., and Bohlke, J. K.: A bacterial method for the nitrogen isotopic analysis of nitrate in seawater and freshwater, Anal Chem, 73, 4145-4415, 10.1021/ac010088e, 2001.
Silbiger, N. J., Donahue, M. J., and Brainard, R. E.: Environmental drivers of coral reef carbonate production and bioerosion: a multi-scale analysis, Ecology, 98, 2547-2560, 10.1002/ecy.1946, 2017.
Silverman, J., Lazar, B., and Erez, J.: Community metabolism of a coral reef exposed to naturally varying dissolved inorganic nutrient loads, Biogeochemistry, 84, 67-82, 2007.
Silverman, J., Lazar, B., Cao, L., Caldeira, K., and Erez, J.: Coral reefs may start dissolving when atmospheric CO2 doubles, Geophys Res Lett, 36, 2009.
Smith, J. E., Runcie, J. W., and Smith, C. M.: Characterization of a large-scale ephemeral bloom of the green alga Cladophora sericea on the coral reefs of West Maui, Hawaii, Mar Ecol Prog Ser, 302, 77-91, 2005.
Smith, S. V.: Carbon dioxide dynamics: a record of organic carbon production, respiration, and calcification in the Eniwetok reef flat community, Limnol. Oceanogr, 18, 106-120, 1973.
Smith, S. V., Kimmerer, W. J., Laws, E. A., Brock, R. E., and Walsh, T. W.: Kaneohe Bay sewage diversion experiment: perspectives on ecosystem responses to nutritional perturbation, Pac Sci, 35, 279-395, 1981.
Sparks, R. T., Stone, K., White, D. J., Ross, M., and Williams, I. D.: Maui and Lanai Monitoring Report, Hawaii Department of Land and Natural Resources, Division of Aquatic Resources, Maui, 130 Mahalani Street, Wailuku HI. 96790, 2016.
Storlazzi, C. D., McManus, M. A., Logan, J. B., and McLaughlin, B. E.: Cross-shore velocity shear, eddies and heterogeneity in water column properties over fringing coral reefs: West Maui, Hawaii, Cont Shelf Res, 26, 401-421, 2006.
Storlazzi, C. D., and Jaffe, B. E.: The relative contribution of processes driving variability in flow, shear, and turbidity over a fringing coral reef: West Maui, Hawaii, Estuarine, Coastal and Shelf Science, 77, 549-564, 10.1016/j.ecss.2007.10.012, 2008.

Strong, A. L., Kroeker, K. J., Teneva, L. T., Mease, L. A., and Kelly, R. P.: Ocean Acidification 2.0: Managing our Changing Coastal Ocean Chemistry, Bioscience, 64, 581-592, 10.1093/biosci/biu072, 2014.

Sunda, W. G., and Cai, W.-J.: Eutrophication Induced CO2-Acidification of Subsurface Coastal Waters: Interactive Effects of Temperature, Salinity, and Atmospheric PCO2, Environ Sci Technol, 46, 10651-10659, 10.1021/es300626f, 2012.

Suzuki, A., and Kawahata, H.: Carbon budget of coral reef systems: an overview of observations in fringing reefs, barrier reefs and atolls in the Indo-Pacific regions, Tellus B, 55, 428-444, 10.1034/j.1600-0889.2003.01442.x, 2003.

Swarzenski, P., Dulai, H., Kroeger, K., Smith, C., Dimova, N., Storlazzi, C., Prouty, N., Gingerich, S., and Glenn, C.: Observations of nearshore groundwater discharge: Kahekili Beach Park submarine springs, Maui, Hawaii, Journal of Hydrology: Regional Studies, 10.1016/j.ejrh.2015.12.056, 2016.

Swarzenski, P. W., Storlazzi, C. D., Presto, M. K., Gibbs, A. E., Smith, C. G., Dimova, N. T., Dailer, M. L., and Logan, J. B.: Nearshore morphology, benthic structure, hydrodynamics, and coastal groundwater discharge near Kahekili Beach Park, Maui, Hawaii:, p. 34 p., U.S. Geological Survey Open-File Report 2012–1166. 2012.

Swarzenski, P. W., Dulaiova, H., Dailer, M. L., Glenn, C. R., Smith, C. G., and Storlazzi, C. D.: A geochemical and geophysical assessment of coastal groundwater discharge at select sites in Maui and O'ahu, Hawai'i, in: Groundwater in the Coastal Zones of Asia-Pacific, edited by: Wetzelhuetter, C., Coastal Research Library, Springer Netherlands, 27-46, 2013.

Szmant, A., and Gassman, N. J.: The effects of prolonged "bleaching" on the tissue biomass and reproduction of the reef coral Montastrea annularis, Coral Reefs, 8, 217-224, 1990.

Wiltse, W.: Algal Blooms: Progress Report on Scientific Research. West Maui Watershed Management Project, 1996.

Wooldridge, S. A.: Excess seawater nutrients, enlarged algal symbiont densities and bleaching sensitive reef locations: 1. Identifying thresholds of concern for the Great Barrier Reef, Australia, Mar Pollut Bull, 10.1016/j.marpolbul.2016.04.054, 2016.

Yao, W., and Byrne, R. H.: Simplified seawater alkalinity analysis: use of linear array spectrometers, Deep Sea Research Part I: Oceanographic Research Papers, 45, 1383-1392, 1998.

Yates, K. K., Zawada, D. G., Smiley, N. A., and Tiling-Range, G.: Divergence of seafloor elevation and sea level rise in coral reef ecosystems, Biogeosciences, 14, 1739-1772, 10.5194/bg-14-1739-2017, 2017.

Zeebe, R. E., and Wolf-Gladrow, D. A.: CO_2 in seawater: equilibrium, kinetics, isotopes, Gulf Professional Publishing, 2001.

Zhang, H., and Byrne, R. H.: Spectrophotometric pH measurements of surface seawater at in-situ conditions: absorbance and protonation behavior of thymol blue, Mar Chem, 52, 17-25, 10.1016/0304-4203(95)00076-3, 1996.

Site	*n*TA-*n*DIC Slope	NCC:NCP	r^2
2016-03-16 to 2016-03-19			
S1	0.88	0.78	0.94
S2	0.67	0.50	0.75
S3	0.93	0.88	0.89
S4	0.93	0.87	0.92
2016-03-21 to 2016-03-24			
S1	0.72	0.56	0.78
S2	0.56	0.39	0.77
S3	0.99	0.98	0.95
S4	1.04	1.08	0.94

Table 1

Slope of salinity normalized total alkalinity (*n*TA): salinity normalized dissolved inorganic carbon (DIC), net community calcification: net community production ratio (NCC:NCP=2ΔDIC/(ΔTA-1)) (Suzuki and Kawahata, 2003) and correlation coefficients (r^2).

Figure 1

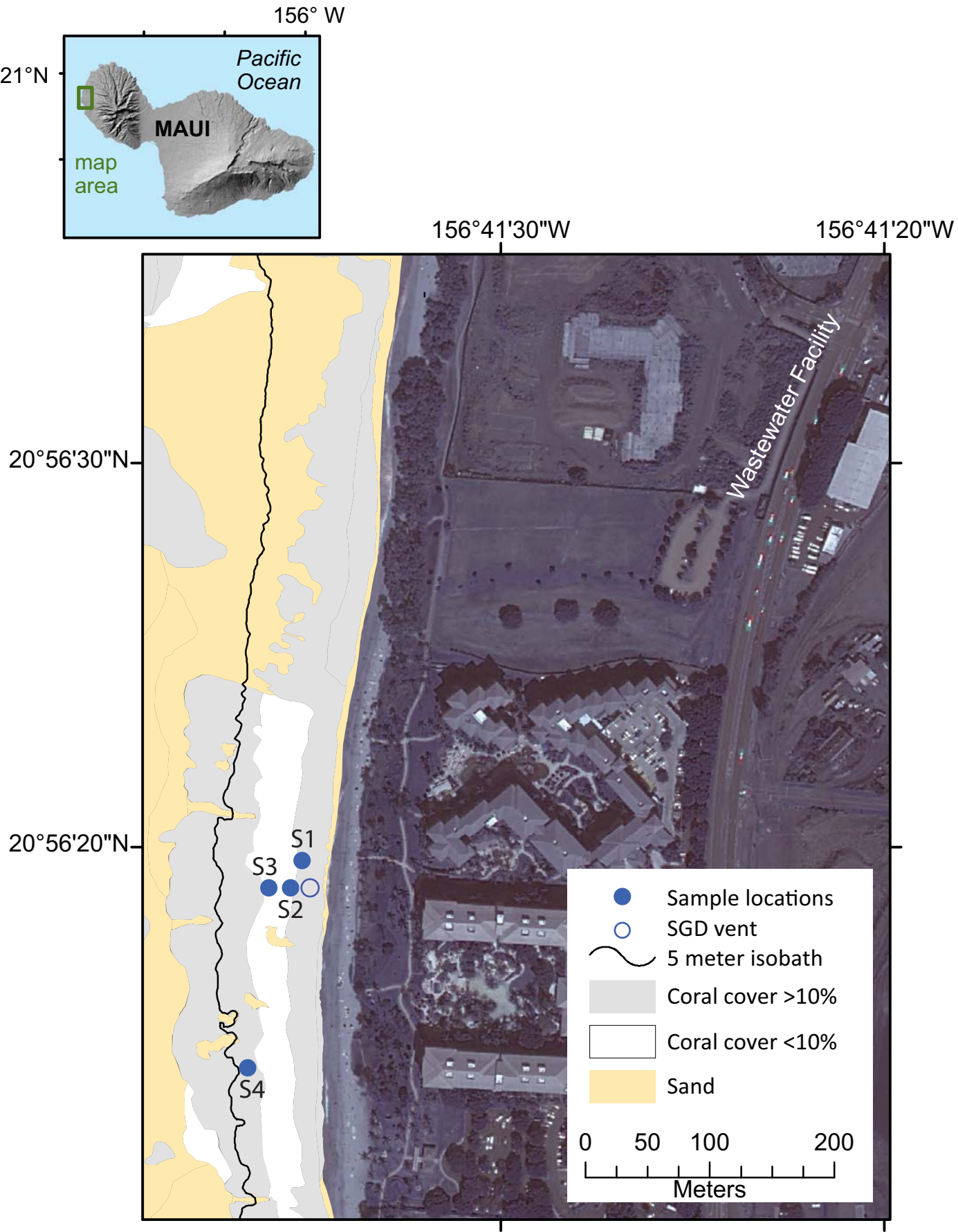
156° W
21°N
Pacific Ocean
MAUI
map area
156°41'30"W
156°41'20"W
20°56'30"N
20°56'20"N
Wastewater Facility
S1
S3
S2
S4
Sample locations
SGD vent
5 meter isobath
Coral cover >10%
Coral cover <10%
Sand
0
50
100
200
Meters

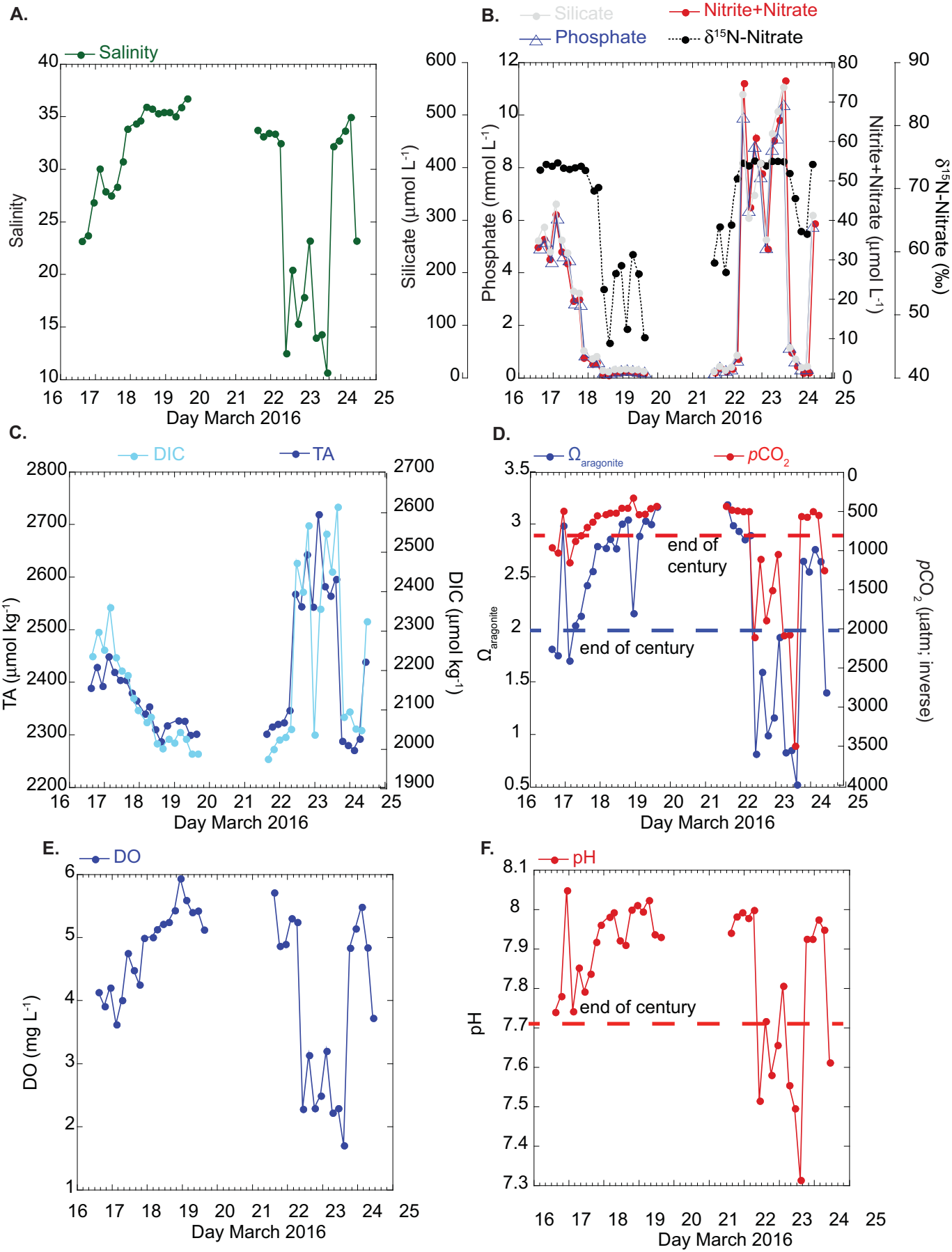
A.
Salinity
Salinity
Day March 2016
B.
Silicate
Phosphate
Nitrite+Nitrate
δ15N-Nitrate
Phosphate (mmol L-1)
Silicate (µmol L-1)
Nitrite+Nitrate (µmol L-1)
δ15N-Nitrate (‰)
Day March 2016
C.
DIC
TA
TA (µmol kg-1)
DIC (µmol kg-1)
Day March 2016
D.
Ωaragonite
pCO2
end of century
end of century
Ωaragonite
pCO2 (µatm; inverse)
Day March 2016
E.
DO
DO (mg L-1)
Day March 2016
F.
pH
end of century
pH
Day March 2016

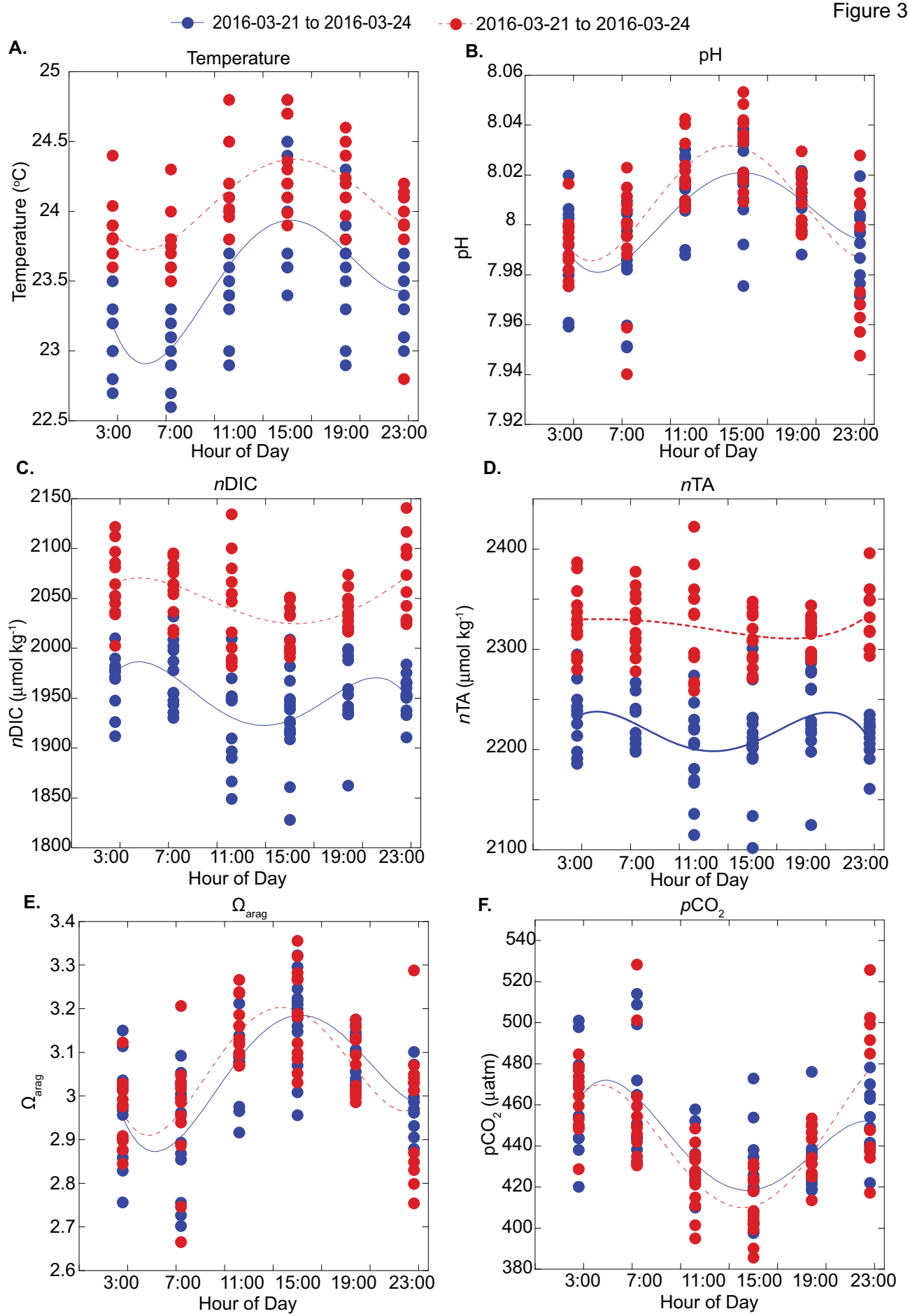
2016-03-21 to 2016-03-24
2016-03-21 to 2016-03-24
A.
Temperature
Temperature (°C)
Hour of Day
B.
pH
pH
Hour of Day
C.
nDIC
nDIC (µmol kg⁻¹)
Hour of Day
D.
nTA
nTA (µmol kg⁻¹)
Hour of Day
E.
Ω arag
Ω arag
Hour of Day
F.
pCO2
pCO2 (µatm)
Hour of Day
3:00
7:00
11:00
15:00
19:00
23:00

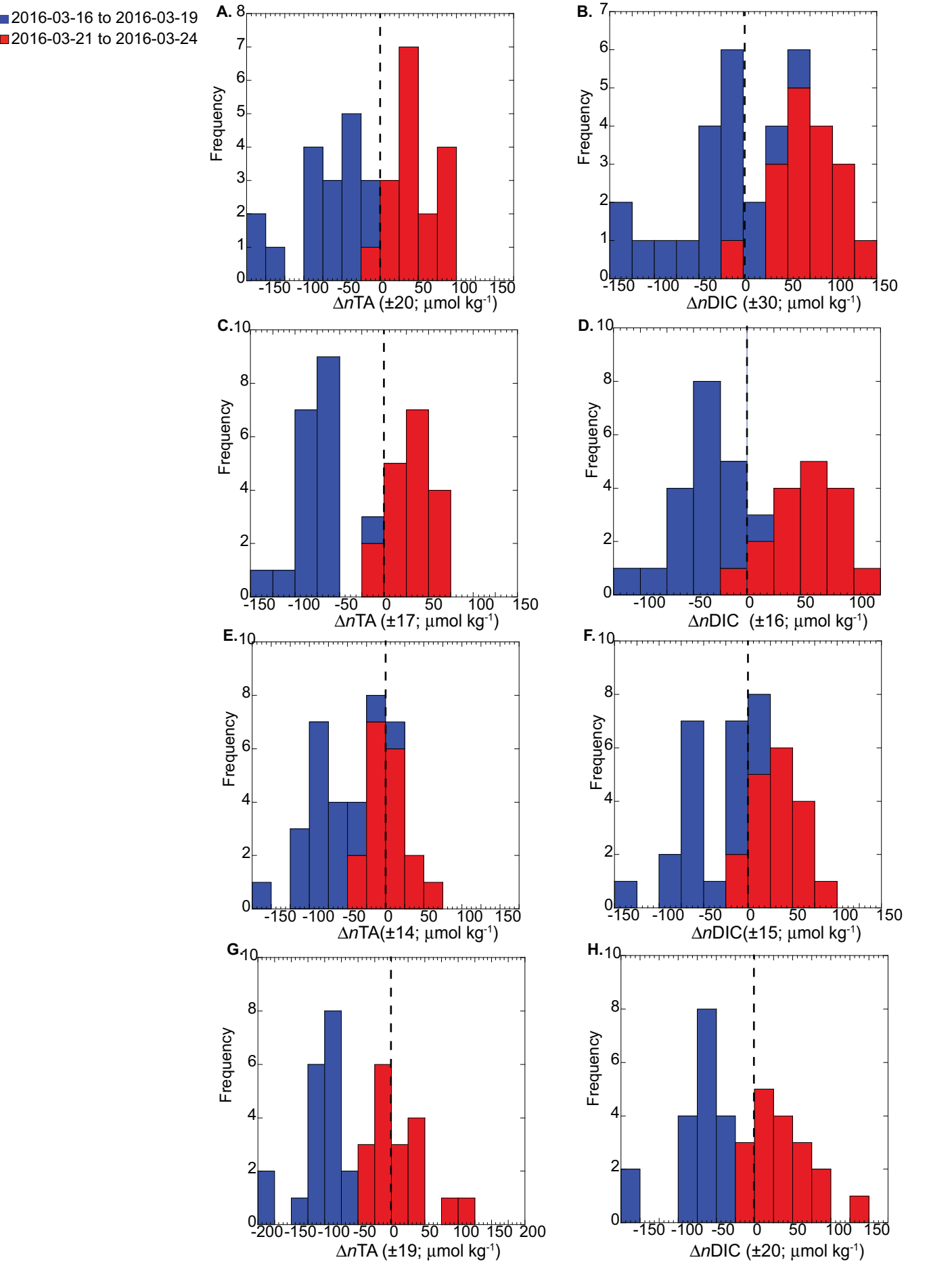
2016-03-16 to 2016-03-19
2016-03-21 to 2016-03-24
A.
Frequency
ΔnTA (±20; µmol kg-1)
B.
Frequency
ΔnDIC (±30; µmol kg-1)
C.
Frequency
ΔnTA (±17; µmol kg-1)
D.
Frequency
ΔnDIC (±16; µmol kg-1)
E.
Frequency
ΔnTA(±14; µmol kg-1)
F.
Frequency
ΔnDIC(±15; µmol kg-1)
G.
Frequency
ΔnTA (±19; µmol kg-1)
H.
Frequency
ΔnDIC (±20; µmol kg-1)

Figure 5

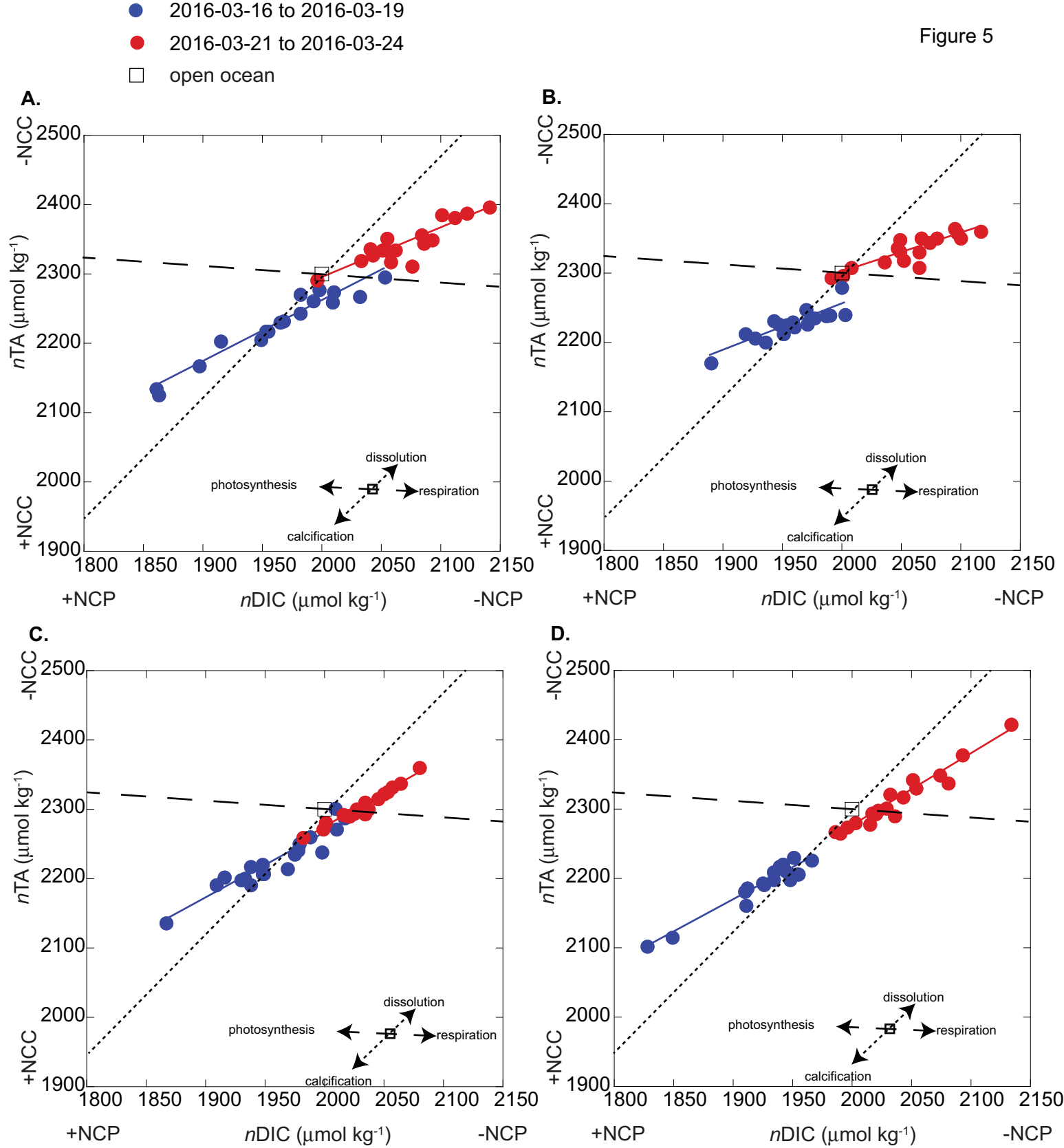
2016-03-16 to 2016-03-19
2016-03-21 to 2016-03-24
open ocean
A.
B.
C.
D.
-NCC
+NCC
nTA (µmol kg-1)
nDIC (µmol kg-1)
+NCP
-NCP
dissolution
photosynthesis
respiration
calcification
2500
2400
2300
2200
2100
2000
1900
1800
1850
1900
1950
2000
2050
2100
2150